Tetrahedron 71 (2015) 3491–3494

Contents lists available at ScienceDirect

Tetrahedron

journal homepage: www.elsevier.com/locate/tet

Pestalotiopsin C, stereochemistry of a new caryophyllene from a fungus of *Trichoderma* sp. and its tautomerization characteristics in solution

He Yu [a], Wen-Xin Li [a], Jing-Chen Wang [a], Qin Yang [a], Hui-Jun Wang [a], Can-Can Zhang [a], Shuang-Shuang Ding [a], Yan Li [b], Hua-Jie Zhu [a,*]

[a] Chinese Center for Chirality, Key Laboratory of Medicinal Chemistry and Molecular Diagnostic of Ministry of Education, College of Pharmacy, Hebei University, Baoding 071002, Hebei, China
[b] State Key Laboratory of Phytochemistry and Plant Resources in West China, Kunming Institute of Botany, Kunming 650204, Yunnan, China

ARTICLE INFO

Article history:
Received 2 February 2015
Received in revised form 15 March 2015
Accepted 16 March 2015
Available online 31 March 2015

Keywords:
Pestalotiopsin C
Trichoderma sp
Optical rotation
ECD
Transition state

ABSTRACT

A new pestalotiopsin C (**1**) with three known compounds (**2**–**4**) are obtained from the fermentation broth of fungus of *Trichoderma* KK19L1 sp. Pestalotiopsin C (**1**) has two atropisomers with mole ratio of 1.2/1 in chloroform at room temperature. Its structure was well established by 1D and 2D NMR, and further confirmed by X-ray diffraction. Its absolute configuration (AC) was determined by comparing its experimental electronic circular dichroism (ECD) and optical rotation (OR) value with the calculated ECD and OR data using quantum methods. The bioactivity of compound **1** was tested against five cell-lines HL-60, SMMC-7721, A-549, MCF-7, SW480, respectively.

1. Introduction

Trichoderma KK19L1 sp. distributes widely in nature. It is well known for its functions in antagonism of plant pathogenic fungi and hyperparasitization,[1] capacity of producing cellulose and other enzymes.[2] Other functions were also reported.[3] Previous studies exhibited that its fermentation moth generally contains anthraquinoes, polyketides, terpenes, alkaloids and other compounds with strong biological activity.[4–6] As part of our ongoing investigation to discover structurally novel and bioactive natural compounds, fermentation of *Trichoderma* KK19L1 sp. was performed, and a new compound was isolated from it. Its planar structure was established by 1D and 2D NMR, such as HMBC and HSQC. Single-crystal X-ray diffraction using Mo radiation confirmed its planar structure and relative configuration. This novel compound has two atropisomers with a ratio of 6:5 in solution. Early reported similar compounds' absolute configuration (AC) was not established although X-ray study was performed.[7] Thus, it's AC was assigned by comparing its experimental optical rotation (OR) and electronic circular dichroism (ECD) with the theoretical OR and ECD at the B3LYP/6-311++G(2d,p)//B3LYP/6-311+G(d) level. Transition state (TS) barriers were well calculated using B3LYP/6-311+G(d) method to explain the reasons of two stable atropisomers existed in solution.

2. Results and discussion

Pestalotiopsin C (**1**) (Fig. 1) was obtained as a colorless crystal from MeOH. ^{1}H NMR and ^{13}C NMR spectrum data of **1** (Table 1,

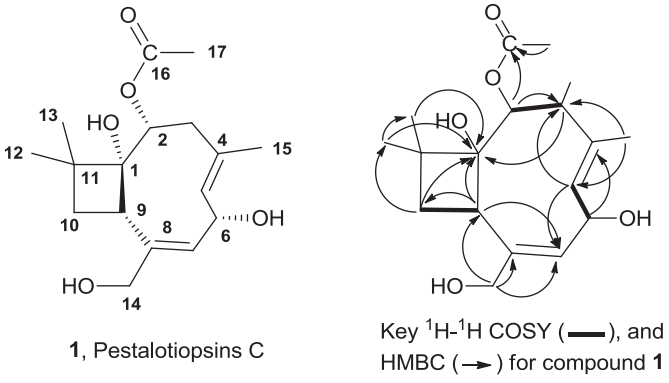

Fig. 1. The structure of compound **1** and its HMBC and H–H COSY.

* Corresponding author. Tel./fax: +86 312 5994812; e-mail address: hjzhu@mail.kib.ac.cn (H.-J. Zhu).

http://dx.doi.org/10.1016/j.tet.2015.03.063
0040-4020/

Table 1
^{1}H and ^{13}C NMR data for compound **1** in methanol-d_4

Set 1			Set 2		
Position	δ_H, multi (J in Hz)	δ_C	Position	δ_H, multi (J in Hz)	δ_C
1		82.78(C)	1		81.35(C)
2	5.26, overlapped	79.36(CH)	2	5.29, overlapped	76.18(CH)
3	1.78, dd (13.8, 10.3) 2.94, dd (13.8, 7.6)	34.93(CH_2)	3	2.33, dd (10.6, 4.2) 2.55, t (11.0)	39.73(CH_2)
4		139.79(C)	4		129.29(C)
5	5.92, d (7.7)	128.82(CH)	5	5.29, overlapped	131.79(CH)
6	4.76, d (7.7)	66.13(CH)	6	4.89, overlapped	66.42(CH)
7	5.99, overlapped	141.79(CH)	7	5.97, overlapped	141.65(CH)
8		133.44(C)	8		136.27(C)
9	3.38, overlapped	45.54(CH)	9	3.22, dd (10.1, 8.4)	40.34(CH)
10	1.59, dd (10.8, 8.8) 2.18, t (11.0)	35.55(CH_2)	10	1.68, dd (12.4, 10.6) 2.10, dd (12.5, 8.0)	33.27(CH_2)
11		40.24(C)	11		40.23(C)
12	1.13, s	24.33(CH_3)	12	1.13, s	23.56(CH_3)
13	1.06, s	23.05(CH_3)	13	1.06, s	26.21(CH_3)
14	3.87, overlapped 4.17, d (10.9)	65.76(CH_2)	14	3.90, overlapped 4.31, d (11.2)	65.52(CH_2)
15	1.83, s	23.92(CH_3)	15	1.95, s	15.97(CH_3)
16		170.76(C)	16		170.61(C)
17	2.04, s	19.95(CH_3)	17	2.04, s	19.98(CH_3)

dissolved in CD_3OD) exhibited two sets of signals with a ratio of 6:5 (^{1}H NMR integration). HPLC analyses using different column (including chiral column like Chiralpak IA , IB , IC and ID) exhibited one sharp signal at 230 nm. It looks not like a dimer since the ratio of the two sets of NMR is not the same (1:1).

The largest possibility is that it has two stable conformations with different relative energy at room temperature. After careful examination, the two sets of NMR spectra were successfully separated from each other (Table 1).

In COSY spectra of set 1, H-5/H-6 spin systems were observed. HMBC spectra exhibited the correlation of H-15 to C-3, and C-5, as well as from H-6 to C-4, allowed the connection of a segment: C-3/C-4/C-5/C-6 with a methyl (Me-15) connected to C-4. The correlations from H-14 to C-7, C-8, C-9, respectively, indicated the $-CH_2OH$ group connected to C-8. HMBC correlations of H-9 to C-7, and H-5 to C-7 allowed the assembly of a segment: C-5/C-6/C-7/C-8/C-9. The planar structure of the four-membered ring was elucidated mainly by the HMBC correlations from H-10 to C-12, C-1, as well as from H-9 to C-1, C-10, C-7, respectively. Me-12 and Me-13 connected to C-11 based on the HMBC correlations from H-12 to C-13, C-1, and H-13 to C-1, respectively. The key correlations of H-2 to C-16, H-17 to C-16, corroborated the carbonyl connected to C-2. These observations, together with the assistance of analysis of other 2D NMR (COSY and HMBC) correlations (Fig. 1), established the planar structure as illustrated below.

The correlations that were found in NMR signals of set 2 were almost the same as those recorded in set 1 (Table 1). This exhibited the two sets of NMR were from one same compound. According to the reported results, it has the similar skeleton to pestalotiopsins A-B, which also have two sets of NMR signals. Therefore, compound **1** was named as pestalotiopsin C. The relative configuration of **1** was finally confirmed by single-crystal X-ray diffraction (Fig. 2) using Mo radiation.

Its AC was well established by comparing the calculated ORs and ECD with the experimental ones. (1*R*,2*R*,6*S*,9*S*)-**1** was used in calculations of both OR and ECD.[8] Totally 32 stable conformations were recorded using MMFF94S force field. These geometries were then optimized at the B3LYP/6-311+G(d) level in the gas phase. The conformers with relative energy in 0–2.5 kcal/mol were used for OR calculations at the B3LYP/6-311++G(2d,p) level. The predicted OR value for (1*R*,2*R*,6*S*,9*S*)-**1** was +222.61 in the gas phase. Once the optimizations were performed at the B3LYP/6-311+G(d) level in methanol using PCM model, the predicted OR value for (1*R*,2*R*,6*S*,9*S*)-**1** was +235.66 at the B3LYP/6-311++G(2d,p)//PCM(methanol)/B3LYP/6-311+G(d) level. The experimental OR values was −182 in methanol. The relative configuration was well established by X-ray. Therefore, its real AC should be (1*S*,2*S*,6*R*,9*R*).

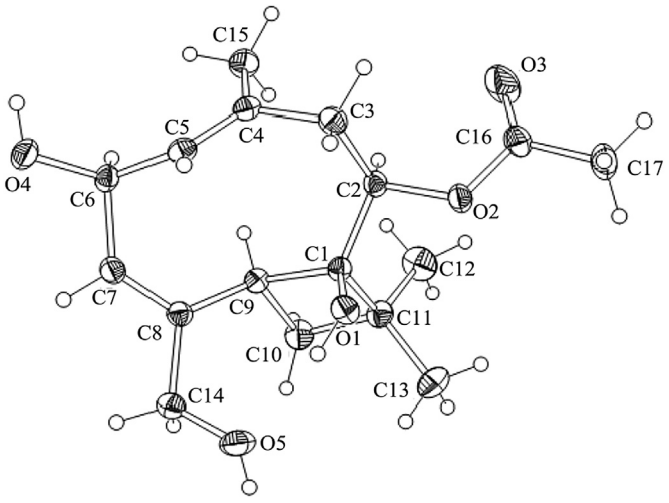

Fig. 2. The X-ray experimental structure.

The AC of C-6 and C-9 could be determined using ECD method too since the two stereogenic centers are close to the chromophore C=C bond.[8] The predicted ECD at the B3LYP/6-311++G(2d,p)//B3LYP/6-311+G(d) level for (1*R*,2*R*,6*S*,9*S*)-**1** exhibited almost a mirror-imagine-like curve of experimental ECD when the half-peak width was 0.5 eV used (Fig. 3). This confirmed the obtained compound (−)-**1** should have (1*S*,2*S*,6*R*,9*R*) AC.

Transition state (TS) analyses were performed at the B3LYP/6-311+G(d) level in the gas phase to understand the phenomena.[9] The predicted TS structure is illustrated below (Fig. 4). Due to rotation of double bond of C(4)=C(5) around two single bonds C3–C4 and C5–C6, this rotation TS barrier was 19.6 kcal/mol using total electronic energy or 19.7 kcal/mol using free energy. This barrier is high enough to block fast rotation of double bond of C(4)=C(5) around the two single bonds C3–C4 and C5–C6, respectively. Namely, one stable conformation cannot convert fast to another

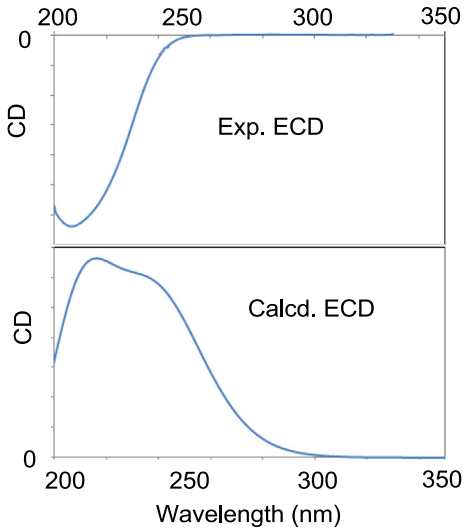

Fig. 3. Experimental ECD for (−)-**1** and predicted ECD for (1*R*,2*R*,6*S*,9*S*)-**1**.

reported in the literature, they were identified as 1-hydroxy-6-methyl-9,10-anthraquinone (**2**),[10] 5-hydroxy-3-hydroxymethyl-2-methyl-7-methoxychromone (**3**)[11] and 4-((2*E*,4*E*)-hexa-2,4-dien-1-yl)-3-((*S*)-2-hydroxypropyl)-furan-2(5H)-one (**4**),[12] respectively.

2.1. Experimental section

Liquid fermentation (120 L) of strain KK19L1 was performed using PDA medium at 28 °C for 20 days. Fermentation broth was extracted with a mixture of EtOAc–MeOH–AcOH (80:15:5) at room temperature for five times. The combined organic layers were filtered by Celite. The organic solvent was removed under a reduced pressure. The residues were subjected to chromatography column using Sephadex LH-20 and silica, repeatedly, to afford the rough sample of pestalotiopsin C(**1**). It recrystallized from MeOH to yield pure **1**.

Pestalotiopsin C(**1**), (4*E*,7*E*) (1*S*,2*S*,6*R*,9*R*)-1,6-dihydroxy-8-(hydroxymethyl)-4,11,11-trimethylbicyclo[7.2.0]undeca-4,7-dien-2-yl acetate. Colorless crystal , $[\alpha]_D^{20}$ −182 (*c* 0.357, MeOH). ^{1}H and

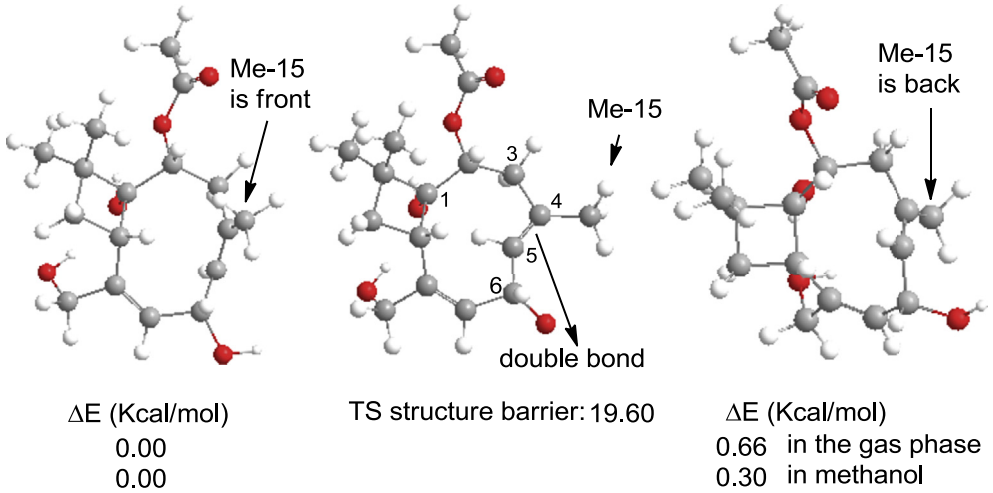

Fig. 4. The most stable conformation (Me-15 is toward the front) and the second most stable conformation (Me-15 is backward).

one at room temperatures. The ratio predicted for the two atropisomers is 3:1 using single point energy (SPE) at the B3LYP/6-311++G(2d,p) level by use of B3LYP/6-311+G(d)-optimized geometry in the gas phase. This ratio is much larger than the experimental one 6:5 (1.2:1). Therefore, the two conformations were further optimized again in methanol at the B3LYP/6-311+G(d) level using PCM model. The energy difference decreased to 0.30 kcal/mol using SPE at the B3LYP/6-311++G(2d,p) level. In this case, the ratio becomes 1.6:1. This is very close to the experimental ratio of 1.2:1. The TS structure and two stable isomers are illustrated below (Fig. 4).

Other three known compounds (Fig. 5) were also obtained. By comparing the observed spectroscopic data with those ^{13}C NMR data are illustrated in Table 1. ESI(+)-MS *m*/*z* 333 $[M+Na]^+$, 643 $[2M+Na]^+$; HRESI(+)-MS *m*/*z* 333.1671 $[M+Na]^+$ (calcd for $C_{17}H_{26}NaO_5$: 333.1672).

X-ray experimental results. Wavelength 0.711 Å; space group $P2_12_12_1$; unit cell dimensions, *a*=11.335 Å, alpha=90°, *b*=11.833 Å, beta=90°, *c*=12.188 Å, gamma=90°. Volume, Z 1634.9 Å^3; Density (calcd) 1.26 g/cm^3; crystal size 0.27 0.26 0.16 mm; completeness, θ=29.93°, 99.0%.

Compound **2**, 1-hydroxy-6-methyl-9,10-anthraquinone. Yellow powder, ^{1}H NMR (600 MHz, $CDCl_3$) δ: 12.54 (1H, s, OH), 8.27 (2H, m, H-5, H-8), 7.79 (1H, m, H-4), 7.62 (1H, m, H-3), 7.27 (1H, m, H-2), 7.09 (1H, d, *J*=7.56 Hz, H-7); ^{13}C NMR (150 MHz, $CDCl_3$) δ: 188.0 (C-9), 182.6 (C-10), 162.8 (C-1), 148.6 (C-6), 134.4 (C-3), 134.1 (C-7),

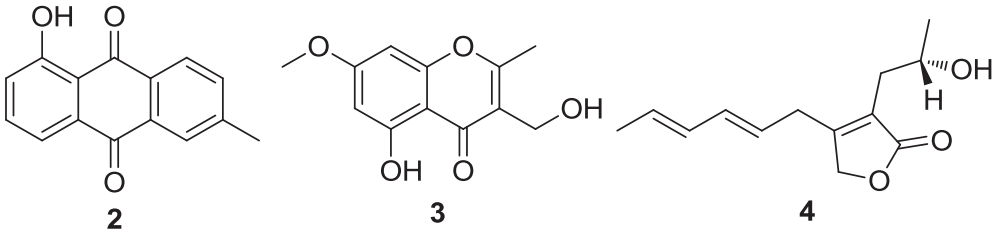

Fig. 5. Structures of compounds **2**, **3** and **4**.

133.6 (C-11), 133.3 (C-14), 133.1 (C-12), 127.3 (C-5), 126.8 (C-8), 120.0 (C-4), 116.1 (C-13), 22.2 (CH_3).

Compound **3**, 5-hydroxy-3-hydroxymethyl-2-methyl-7-metho xychromone. White needle crystal, ^{1}H NMR (600 MHz, $CDCl_3$) δ: 12.54 (1H, s, OH), 6.36 (2H, m, H-6, H-8), 6.42 (2H, d, J=6.6 Hz, CH_2), 3.88 (3H, s, OCH_3), 3.04 (1H, t, J=6.6 Hz, OH), 4.48 (3H, s, CH_3), 1.67 (2H, s, CH_2); ^{13}C NMR (150 MHz, $CDCl_3$) δ: 182.3 (C-4), 165.6 (C-7), 164.6 (C-2), 162.1 (C-5), 157.7 (C-8a), 118.3 (C-3), 104.9 (C-4a), 98.1 (C-6), 92.3 (C-8), 56.7 (CH_2OH), 55.8 (OCH_3), 17.9 (CH_3)。

Compound **4**, 4-((2*E*,4*E*)-hexa-2,4-dien-1-yl)-3-((*S*)-2-hydroxypropyl)- furan-2(5H)-one. Oil, $[\alpha]_D^{20}$ +6.1 (*c* 0.25, $CHCl_3$), ^{1}H NMR (600 MHz, $CDCl_3$) δ, 5.98 (2H, overlapped, H-3′, H-4′), 5.66 (1H, m, H-2′), 5.41 (1H, m, H-5′), 4.69 (2H, s, H-5), 4.03 (1H, m, H-2″), 3.19 (2H, d, J=8.02 Hz H_2-6′), 2.43 (2H, m, H-1″), 1.72 (3H, d, J=10.2 Hz, H_3-1′), 1.20 (3H, d, J=8.36 Hz, H_3-3″); ^{13}C NMR (150 MHz, $CDCl_3$) δ: 175.9 (C-2), 161.4 (C-3), 134.0 (C-4′), 130.3 (C-3′), 130.1 (C-2′), 124.5 (C-4), 123.6 (C-5′), 71.8 (C-5), 66.3 (C-2″), 33.2 (C-1″), 30.3 (C-6′), 23.3 (C-3″), 17.9 (C-1′).

2.2. Computational section

Conformational searches were performed for (1*R*,2*R*,6*S*,9*S*)-**1** using MMFF54S force field, all 32 conformations were found and used in further optimizations at the B3LYP/6-311+G(d) level in the gas phase. The low energy conformations (total 10, 0–2.5 kcal/mol) were used for OR and ECD computations at the B3LYP/6-311++G(2d,p) level in the gas phase. Boltzmann statistics were used for OR and ECD calculations.

TS calculations were performed at the B3LYP/6-311+G(d) level in the gas phase. The predicted TS structures were used for frequency analysis to ensure that the predicted TS structure is the expected ones. All of imaginary frequency (negative data) were predicted with correct vector directions in the TS structures. The ratio of two stable conformations was computed using the two stable conformations energy. Two ratios were computed. The first one is to use SPE predicted at the B3LYP/6-311++G(2d,p) level using B3LYP/6-311+G(d)-optimized geometry in the gas phase. The 0.66 kcal/mol energy difference was obtained between the two conformations, and this exhibited that they would have the ratio of 3:1. The second one is to use SPE obtained at the B3LYP/6-311++G(2d,p) level by use of the B3LYP/6-311+G(d)-optimized geometry in solution by PCM model. In this case, the energy difference is 0.30 kcal/mol, therefore, the ratio became 1.6:1.

Its cytotoxicity was tested using MTS method. Unfortunately, the IC_{50} tested for five cell-lines, HL-60, SMMC-7721, A-549, MCF-7, SW480, respectively, were larger than 40 ug/mL, it had almost no obvious cytotoxicity against the tumor-cell lines.

Acknowledgements

H.J. Zhu thanks the financial support from Hebei University.

Supplementary data

Supplementary data related to this article can be found at http://dx.doi.org/10.1016/j.tet.2015.03.063.

References and notes

1. (a) Ghisalberti, E. L.; Sivthamparam, K. *Soil Biol. Biochem.* **1991**, *23*, 1011–1020; (b) Claydon, N.; Allan, M. *Trans. Br. Mycol. Soc.* **1987**, *88*, 503–513; (c) Smith, V. L.; Wilcox, W. F.; Harman, G. E. *Phytopath* **1990**, *80*, 880–885; (d) Papavizas, G. C. *Ann. Rev. Phytopathol.* **1985**, *23*, 23–54.
2. Kubicek, C. P.; Eveleigh, D. E.; Esterbauer, H.; Steiner, W.; Kubicek-Pranz, E. M. *Roy. Soc. Chem.* **1990**, 47–60.
3. (a) Yedidia, I.; Benhamou, N.; Kapulnik, Y.; Chet, I. *Plant Physiol. Biochem.* **2000**, *38*, 863–873; (b) Yedidia, I.; Shoresh, M.; Kerem, Z.; Benhamou, N.; Kapulnik, Y.; Chet, I. *Appl. Environ. Microbiol.* **2003**, *69*, 7343–7353.
4. (a) Evidente, A.; Cabras, A.; Maddau, L.; Serra, S.; Andolfi, A.; Motta, A. J. *Agric. Food Chem.* **2003**, *51*, 6957–6960; (b) Pruksakorn, P.; Arai, M.; Kotoku, N.; Vilcheze, C.; Baughn, A. D.; Moodley, P.; Jacobs, W. R., Jr.; Kobayashi, M. *Bioorg. Med. Chem. Lett.* **2010**, *20*, 3658–3663; (c) Ding, G.; Chen, L.; Chen, A.; Tian, X.; Chen, X.; Zhang, H.; Chen, H.; Liu, X. Z.; Zhang, Y.; Zou, Z. M. *Fitoterapia* **2012**, *83*, 541–544.
5. (a) Seephonkai, P.; Kongsaeree, P.; Prabpai, S.; Isaka, M.; Thebtaranonth, Y. *Org. Lett.* **2006**, *8*, 3073–3075; (b) Li, G. H.; Yang, Z. S.; Zhao, P. J.; Zheng, X.; Luo, S. L.; Sun, R.; Niu, X. M.; Zhang, K. Q. *Phytochem. Lett.* **2011**, *4*, 86–88; (c) Liu, S. Y.; Lo, C. T.; Shibu, M. A.; Leu, Y. L.; Jen, B. Y.; Peng, K. C. *J. Agric. Food Chem.* **2009**, *57*, 7288–7292.
6. (a) Hosotani, N.; Kumagai, K.; Honda, S.; Ito, A.; Shimatani, T.; Saji, I. *J. Antibiot.* **2007**, *60*, 184–190; (b) Wu, S. H.; Zhao, L. X.; Chen, Y. W.; Huang, R.; Miao, C. P.; Wang, J. *Chem. Biodiversity* **2011**, *8*, 1717–1723; (c) Neumann, K.; Abdel-Lateff, A.; Wright, A. D.; Kehraus, S.; Krick, A.; König, G. M. *Eur. J. Org. Chem.* **2007**, *14*, 2268–2275.
7. Maurizio, P.; Fumio, S.; Hiroyuki, K.; Jun, U.; Shigeo, Y. *J. Org. Chem.* **1996**, *61*, 2122–2124.
8. (a) Zhu, H. J. *Organic Stereochemistry—Experimental and Theoretical Methods*; Wiley-VCH: Weinheim, Germany, 2015, Chapter 4, p87; (b) Zhu, H. J.; Li, W. X.; Hu, D. B.; Wen, M. L. *Tetrahedron* **2014**, *70*, 8236–8243; (c) Hu, D. B.; Li, W. X.; Zhao, Z. Z.; Feng, T.; Yin, R. H.; Li, Z. H.; Liu, J. K.; Zhu, H. J. *Tetrahedron Lett.* **2014**, *55*, 6530–6533; (d) Li, Q. M.; Ren, J.; Shen, L.; Bai, B.; Li, Q. M.; Liu, X. C.; Wen, M. L.; Zhu, H. J. *Tetrahedron* **2013**, *69*, 3067–3074; (e) Ren, J.; Li, G. L.; Shen, L.; Zhang, G. L.; Nafie, L.; Zhu, H. J. *Tetrahedron* **2013**, *69*, 10351–10356; (f) Ding, H. G.; Li, M. G.; Zhao, J. Y.; Ren, J.; Huang, R.; Xie, M. J.; Cui, X. L.; Zhu, H. J.; Wen, M. L. *Chem.-A J. Eur.* **2010**, *16*, 3902–3905.
9. (a) Zhu, H. J. *Modern Organic Stereochemistry*; Science: China, 2009, Chapter 5; (b) Xiao, W. L.; Lei, C.; Ren, J.; Liao, T. G.; Pu, J. X.; Pittman, C. U.; Lu, Y.; Zheng, Y. T.; Zhu, H. J.; Sun, H. D. *Chem.-A J. Eur.* **2008**, *14*, 11584–11592; (c) Li, L. C.; Jiang, J. X.; Ren, J.; Ren, Y.; Pittman, C. U.; Zhu, H. J. *Eur. J. Org. Chem.* **2006**, 1981–1990.
10. Danielsen, K. *Acta Chem. Scand.* **1996**, *50*, 954–957.
11. Liu, T.; Li, Z. L.; Wang, Y.; Tian, L.; Pei, Y. H.; Hua, M. H. *J. Shenyang Pharm. Univ.* **2012**, *29*, 93–97.
12. Almassi, F.; Ghisalberti, E. L.; Narbey, M. J. *J. Nat. Prod.* **1991**, *54*, 396–402.